

Analysis of the $^{16}\text{C}(d,p)^{17}\text{C}$ reaction from microscopic ^{17}C wave functions

Le Hoang Chien^{1,2,3,*} and P. Descouvemont^{1,†}

¹*Physique Nucléaire Théorique et Physique Mathématique, C.P. 229,
Université Libre de Bruxelles (ULB), B 1050 Brussels, Belgium*

²*Department of Nuclear Physics, Faculty of Physics and Engineering Physics,
University of Science, Ho Chi Minh City, Vietnam*

³*Vietnam National University, Ho Chi Minh City, Vietnam*

(Dated: September 18, 2023)

We present a semi-microscopic study of the $^{16}\text{C}(d,p)^{17}\text{C}$ transfer reaction. The ^{17}C overlap integrals and spectroscopic factors are obtained from a microscopic cluster model, involving many $^{16}\text{C} + n$ configurations. This microscopic model provides a fair description of the ^{17}C bound-state energies. The $^{16}\text{C} + d$ scattering wave functions are defined in the CDCC method, where the deuteron breakup is simulated by pseudostates. The transfer cross sections are in good agreement with recent data. We confirm the $^{16}\text{C}(2^+) + n$ structure of the ground state, and show that deuteron breakup effects have a significant influence on the cross sections. We study the $^{17}\text{C}(p,d)^{16}\text{C}$ reverse reaction and suggest that the cross section to the 2^+ state should be large. A measurement of the ground-state cross section would provide a strong test of the microscopic wave functions.

I. INTRODUCTION

The physics of exotic nuclear is one of the main interests in modern nuclear physics [1, 2]. Exotic nuclei are located near the drip lines and therefore present a low breakup threshold, and a small number of bound states. They can be seen as a core nucleus (which may be in an excited state) surrounded by one or two nucleon(s). The recent development of radioactive beams [3] provides helpful information about the structure of exotic nuclei. The analysis of these data require models for the structure of the nucleus, as well as for the reaction process.

Over the last 20 years, the ^{17}C nucleus has been investigated in several works. From a Coulomb breakup experiment, Datta Pramanik *et al.* [4] concluded that the ground state has a spin $3/2^+$ and present a $^{16}\text{C}(2^+) + n$ structure. The study of excited states was performed by Elekes *et al.* [5] by inelastic scattering on a proton target, and by Bohlen *et al.* [6] who used a three-neutron transfer reaction at high energies. Negative-parity states were observed from β -delayed neutron emission of ^{17}B [7]. Satou *et al.* [8] observed several unbound states from proton inelastic scattering, and concluded on the existence of narrow $7/2^+$ and $9/2^+$ resonances are low energies. The lifetime of excited states was investigated by Smalley *et al.* [9] from a one-neutron knockout reaction on ^{18}C . Very recently, this technique was also used by Kim *et al.* [10] who concluded on the existence of a $5/2_2^+$ state, and suggested low-energy negative parity resonances.

On the theoretical side, various techniques have been used to describe the spectroscopy of ^{17}C , in particular the multi channel algebraic scattering (MCAS) model [11], the no-core shell model [9] or large-scale shell model calculations [10]. In Refs. [12, 13], the ^{17}C nucleus was

described in the Resonating Group Method (RGM, see Refs. [14, 15]). In that approach, the ^{17}C wave functions are obtained from a microscopic Hamiltonian, with the cluster approximation. In this way, the 17-nucleon antisymmetrization is exactly taken into account. This technique is well adapted to weakly bound nuclei, where the description of the relative wave function at large distances is a fundamental issue. The RGM provides the overlap integrals and the spectroscopic factors, which are necessary ingredients to the (d,p) transfer cross sections [16]. No further parameter or renormalization factor is necessary, in contrast with the Distorted Wave Born Approximation (DWBA) method [17], where the overlap integral is approximated from the simple potential model, and where the spectroscopic factor is an adjustable parameter.

An efficient tool to investigate the spin of nuclear states is provided by (d,p) reactions, where a neutron is transferred from the deuteron to the target [18]. The cross sections are known to be very sensitive to the target+neutron angular momentum [17]. This technique was used recently by Pereira-López *et al.* in a $^{16}\text{C}(d,p)^{17}\text{C}$ experiment [19]. The authors measured the transfer cross sections to the ^{17}C $1/2^+$ and $5/2^+$ excited states, as well as the sum of the three bound states. Owing to its dominant $^{16}\text{C}(2^+) + n$ structure, the ^{17}C ground state presents a small spectroscopic factor in the $^{16}\text{C}(0^+) + n$ channel, and therefore the corresponding cross section could not be separated.

In the present work, our goal is to analyze the $^{16}\text{C}(d,p)^{17}\text{C}$ reaction by using microscopic ^{17}C wave functions. In the standard DWBA treatment of (d,p) reactions [17], the residual nucleus is described by a potential-model wave function, which is renormalized by a spectroscopic factor to include missing effects, such as the antisymmetrization or the influence of core excited states. This semi-microscopic approach to transfer reactions has been developed in Ref. [20], and we refer to this reference for more detail.

* chienlhphys@gmail.com

† pierre.descouvemont@ulb.be

As the deuteron projectile is weakly bound, breakup effects in the $^{16}\text{C} + d$ scattering wave functions are expected to be important. This problem is addressed by using the Continuum Discretized Coupled Channel (CDCC) method (see Ref. [21] for a review), where the three-body continuum is simulated by pseudostates in the $p+n$ system. This technique is well known, and has been used for many systems. It is particularly well adapted to exotic nuclei, where the breakup threshold energy is low, and where breakup effects are expected to be important (see, for example, Refs. [22, 23]).

The paper is organized as follows. In Section II, we present a brief outline of the model, which is divided in two parts. In the first part, we discuss the RGM ^{17}C wave functions, in particular the overlap integrals and the spectroscopic factors. The second part is focused on the $^{16}\text{C} + d$ scattering wave functions, defined in the CDCC framework. We also provide information on the calculation of the transfer cross sections. The results on the ^{17}C spectroscopy and on the $^{16}\text{C}(d,p)^{17}\text{C}$ cross sections are presented in Sec. III. Conclusions and outlook are discussed in Sec. IV.

II. THE MODEL

A. The Resonating Group Method

Our goal is to describe the ^{17}C wave functions in a microscopic approach. In a A -nucleon system ($A = 17$), the Hamiltonian is given by

$$H_{17} = \sum_{i=1}^A t_i + \sum_{i<j=1}^A v_{ij}, \quad (1)$$

where t_i is the kinetic energy of nucleon i , and v_{ij} is a nucleon-nucleon interaction, including central and spin-orbit components. The Coulomb force is treated exactly. In the Resonating Group Method, the wave functions are defined at the cluster approximation and involve internal wave functions of the clusters, as well as a relative function. The internal wave functions are defined in the shell model. For the ^{17}C nucleus, the RGM wave function associated with Hamiltonian H_{17} reads

$$\Psi_{17}^{JM\pi} = \mathcal{A} \frac{1}{\rho} \sum_c \varphi_c^{JM\pi} g_c^{J\pi}(\rho), \quad (2)$$

where \mathcal{A} is the A -nucleon antisymmetrizer, $\boldsymbol{\rho} = (\rho, \Omega_\rho)$ is the relative coordinate between ^{16}C and the neutron, and $g_c^{J\pi}(\rho)$ are the radial wave functions. The channel functions $\varphi_c^{JM\pi}$ are given by

$$\varphi_c^{JM\pi} = \left[[\phi_{16}^{I_1} \otimes \phi_n]^I \otimes Y_\ell(\Omega_\rho) \right]^{JM}, \quad (3)$$

where $\phi_{16}^{I_1}$ are shell-model wave functions of ^{16}C (with an oscillator parameter b , chosen here as $b = 1.6$ fm), ϕ_n is a

neutron spinor, and index c stands for $c = (\ell, I_1, I)$. We adopt the same conditions as in Ref. [13], where ^{16}C is described by all Slater determinants involving four protons in the p shell, and two neutrons in the sd shell. This leads to 990 Slater determinants to describe the ground state and several excited states (see Ref. [13] for detail).

In the calculation of transfer cross sections, the relevant quantities are the overlap integrals [24, 25], defined as

$$I_c^{J\pi}(\rho) = \frac{1}{\rho} \langle \varphi_c^{JM\pi} | \Psi_{17}^{JM\pi} \rangle, \quad (4)$$

which are defined for each channel c . This definition provides the spectroscopic factor from

$$S_c^{J\pi} = \int [I_c^{J\pi}(\rho)]^2 d\rho. \quad (5)$$

The relative functions $g_c^{J\pi}(\rho)$ must be determined from the Schrödinger equation associated with Hamiltonian (1). In practice, we use the Generator Coordinate Method (GCM, see Refs. [15, 26]), where $g_c^{J\pi}(\rho)$ is expanded as

$$g_c^{J\pi}(\rho) = \int dR f_c^{J\pi}(R) \Gamma_\ell(\rho, R). \quad (6)$$

In this equation, R is the generator coordinate, and the projected Gaussian function $\Gamma_\ell(\rho, R)$ is defined as

$$\Gamma_\ell(\rho, R) = \left(\frac{\mu}{\pi b^2} \right)^{3/2} \exp\left(-\frac{\mu}{2b^2}(\rho^2 + R^2)\right) i_\ell\left(\frac{\mu\rho R}{b^2}\right), \quad (7)$$

μ being the reduced mass and $i_\ell(x)$ a spherical Hankel function. With expansion (6), the total wave function (2) can be written as a superposition of projected Slater determinants [26], well adapted to systematic numerical calculations. In the GCM, the calculation of the radial functions $g_c^{J\pi}(\rho)$ is therefore replaced by the calculation of the generator functions $f_c^{J\pi}(R)$.

The Gaussian asymptotic behaviour (7) is corrected with the microscopic R -matrix method [27] for scattering states as well as for bound states. This issue is important for weakly bound states, where the wave function presents a slow decrease at large distances. The technique to derive the overlap integrals in the RGM is explained, for example, in Refs. [20, 28]. It is based on the calculation of the overlap kernels between GCM basis functions.

The Asymptotic Normalization Coefficient (ANC) $C_c^{J\pi}$ in channel c is defined from the long-range limit of the overlap integral as

$$I_c^{J\pi}(\rho) \longrightarrow C_c^{J\pi} W_{-\eta_c, \ell+1/2}(2k_c\rho), \quad (8)$$

where k_c and η_c are the wave number and Sommerfeld parameter in channel c , and $W_{ab}(x)$ is the Whittaker function [29]. The ANC depends on the wave function at

large distances, whereas the spectroscopic factor probes the inner part of the wave function. Both quantities are therefore complementary. Notice that the asymptotic forms of the relative wave functions $g_c^{J\pi}(\rho)$ and of the overlap integrals $I_c^{J\pi}(\rho)$ are identical.

B. $^{16}\text{C} + d$ and $^{17}\text{C} + p$ scattering wave functions

In the entrance channel, the $^{16}\text{C} + d$ scattering wave functions are defined in the CDCC formalism, which simulates breakup effects of the deuteron by $p + n$ pseudostates [21]. The three-body Hamiltonian is defined as

$$H = H_0(\mathbf{r}) + T_R + V_{pC} + V_{nC}, \quad (9)$$

where H_0 is the $p+n$ Hamiltonian, T_R the $^{16}\text{C} + d$ kinetic energy, and V_{pC} and V_{nC} are optical potentials between the nucleons and ^{16}C . In Eq. (9), \mathbf{r} is the $p + n$ relative coordinate, and \mathbf{R} is associated with the $^{16}\text{C} + d$ system.

In the CDCC method, $p + n$ wave functions are obtained from

$$H_0\phi_k^{\ell m}(\mathbf{r}) = E_k^\ell\phi_k^{\ell m}(\mathbf{r}), \quad (10)$$

where k is the excitation level, and ℓ the angular momentum. This equation provides one bound state ($E_1^0 < 0$), associated with the deuteron, and positive-energy states ($E_k^\ell > 0$), referred to as pseudostates, which represent approximations of the continuum. The $^{16}\text{C} + d$ wave functions are then defined as

$$\Psi_i^{JM\pi} = \frac{1}{R} \sum_{\gamma} u_{\gamma}^{J\pi}(R) [\phi_k^{\ell}(\mathbf{r}) \otimes Y_L(\Omega_R)]^{JM}, \quad (11)$$

where L is the relative orbital momentum between ^{16}C and d , and where index γ stands for $\gamma = (\ell, k, L)$. The summation over the pseudostates (ℓ, k) must be truncated at some ℓ_{\max} and E_{\max} values, which are chosen large enough so that the expansion (11), and the associated cross sections converge.

The radial functions $u_{\gamma}^{J\pi}(R)$ and the associated scattering matrices at a center-of-mass (c.m.) energy E are obtained from the standard coupled-channel system

$$(T_L(R) + E_k^\ell - E)u_{\gamma}^{J\pi}(R) + \sum_{\gamma'} V_{\gamma, \gamma'}^{J\pi}(R)u_{\gamma'}^{J\pi}(R) = 0, \quad (12)$$

with

$$T_L(R) = -\frac{\hbar^2}{2\mu} \left(\frac{d^2}{dR^2} - \frac{L(L+1)}{R^2} \right). \quad (13)$$

The coupling potentials $V_{\gamma, \gamma'}^{J\pi}(R)$ are obtained from matrix elements of the optical potentials $V_{pC} + V_{nC}$ [21]. Finally, system (12) is solved with the R -matrix method [27, 30] on a Lagrange mesh [31] which provides the scattering matrices and the radial wave functions for all $J\pi$ values.

For the $^{17}\text{C} + p$ exit channel, the scattering wave functions are defined from an optical potential as

$$\Psi_f^{JM\pi} = \frac{1}{R'} u_f^{J\pi}(R') \left[[\Psi_{17} \otimes \phi_p]^{I_f} \otimes Y_{L_f}(\Omega_{R'}) \right]^{JM}, \quad (14)$$

where \mathbf{R}' is the $^{17}\text{C} + p$ relative coordinate, and where L_f and I_f are the angular momentum and the channel spin in the exit channel. Function $u_f^{J\pi}(R')$ is obtained from the Schrödinger equation

$$(T_{L_f}(R') + V_{\text{opt}}(R') - E_f)u_f^{J\pi}(R') = 0 \quad (15)$$

which involves the optical potential $V_{\text{opt}}(R')$, associated with $^{17}\text{C} + p$ (E_f is the scattering energy in this channel).

C. Transfer scattering matrices

We follow the method of Ref. [20], and refer the reader to this reference for detail. The (d, p) transfer scattering matrix from an initial state i to a final state f is defined by

$$U_{i,f}^{J\pi} = -\frac{i}{\hbar} \langle \Psi_f^{J\pi} | V_{pn} + \Delta V | \Psi_i^{J\pi} \rangle, \quad (16)$$

where we use the post representation, and where ΔV is the remnant potential [17, 18]. A difficulty associated with definition (16) is that the coordinates (\mathbf{R}, \mathbf{r}) in the entrance channel are different from those in the exit channel $(\mathbf{R}', \mathbf{r}')$. In practice, \mathbf{r} and \mathbf{r}' are expressed from \mathbf{R} and \mathbf{R}' (see, for example, Ref. [32] for detail). Using definitions (11) and (14) of the scattering wave functions, the transfer scattering matrix (16) can be reformulated as

$$U_{i,f}^{J\pi} = -\frac{i}{\hbar} \sum_{\gamma} \int u_{\gamma}^{J\pi}(R) K_{\gamma}^{J\pi}(R, R') u_f^{J\pi}(R') R R' dR dR'. \quad (17)$$

For a given ^{17}C state, the transfer kernel is given by

$$K_{\gamma}^{J\pi}(R, R') = \mathcal{J} \sum_c \langle [\phi_k^{\ell}(\mathbf{r}) \otimes Y_{L_i}(\Omega_R)]^J | V_{pn} + \Delta V | [I_c(\mathbf{r}') \otimes Y_{L_f}(\Omega_{R'})]^J \rangle, \quad (18)$$

where \mathcal{J} is the Jacobian, and $I_c(\mathbf{r}')$ are the overlap functions defined in Eq. (4). In Eq. (17), the summation over index γ arises from the CDCC expansion of the $^{16}\text{C} + d$ scattering wave functions. The use of a Lagrange mesh to define the radial functions $u_{\gamma}^{J\pi}(R)$ makes the numerical calculations of the double integrals (17) rather fast [32]. The R -matrix channel radius is chosen large enough to guarantee the convergence.

III. THE $^{16}\text{C}(d,p)^{17}\text{C}$ TRANSFER REACTION

A. Overlap integrals of ^{17}C

The conditions of the calculations are as in Ref. [13], where a multichannel $^{16}\text{C} + n$ RGM calculation is performed with all $(\pi p)^4(\nu sd)^2$ ^{16}C configurations (990 Slater determinants). The spectra of ^{16}C and ^{17}C given in Ref. [13] agree reasonably well with experiment. We use the Volkov $V2$ interaction, complemented by a zero-range spin-orbit force. The Majorana parameter is $M = 0.668$, and the spin-orbit amplitude is $31.3 \text{ MeV}\cdot\text{fm}^5$. With these parameters, $3/2^+$, $1/2^+$ and $5/2^+$ states are obtained below the $^{16}\text{C} + n$ threshold, in agreement with experiment. For the calculation of the overlap integrals and of the spectroscopic factors, a slight readjustment of M is introduced in order to reproduce exactly the experimental binding energies (-0.734 , -0.517 and -0.402 MeV, respectively).

A useful information on the structure of a nucleus is provided by the rms radius, defined in a translation-invariant form as

$$\langle r^2 \rangle = \frac{1}{A} \langle \Psi_{17}^{J\pi} | \sum_{i=1}^A (\mathbf{r}_i - \mathbf{R}_{\text{c.m.}})^2 | \Psi_{17}^{J\pi} \rangle, \quad (19)$$

where $\mathbf{R}_{\text{c.m.}}$ is the center-of-mass of the system. The rms radius of the ^{16}C core is given by the shell-model value $\sqrt{\langle r^2 \rangle} = \sqrt{73/32}b = 2.42 \text{ fm}$ with $b = 1.6 \text{ fm}$ (see Sec. II.A).

In Fig. 1, we show the overlap integrals for the three bound states, and we provide the corresponding spectroscopic factors and ANC in Table I. Let us first discuss the $3/2^+$ ground state shown in Fig. 1(a). This ^{17}C state is essentially described by a $^{16}\text{C}(2^+) + n$ configuration. The overlap integral in the $^{16}\text{C}(0^+) + n$ channel is quite small. The main contribution to the spectroscopic factor comes from the $(I, \ell) = (3/2, 2)$ channel with $S = 0.97$. As mentioned in Ref. [19], the $^{16}\text{C}(d,p)^{17}\text{C}$ cross section to the ground state is expected to be small, owing to the small spectroscopic factor in this channel ($S = 5.2 \times 10^{-3}$). The ground-state radius is in reasonable agreement with a recent experiment ($2.68 \pm 0.05 \text{ fm}$) [33], where interaction cross sections are analyzed in the Glauber model.

In contrast, the $1/2^+$ first excited state has a dominant $^{16}\text{C}(0^+) + n$ structure. The low binding energy (-0.517 MeV) and the angular momentum $\ell = 0$ suggest a halo structure, which is supported by the large ANC value and by the large rms radius. The GCM radius corresponds to a $^{16}\text{C} + n$ distance of 6.10 fm (in comparison, this distance is 4.78 fm for the ground state). The $^{16}\text{C}(2^+) + n$ channel plays a minor role, essentially at short distances.

The $5/2^+$ second excited state is more complex, since similar overlap integrals are obtained in the $^{16}\text{C}(0^+) + n$ and $^{16}\text{C}(2^+) + n$ channels. Notice that the calculation involves many other $^{16}\text{C} + n$ channels, which have an impact on the ^{17}C wave functions (2). However, the cor-

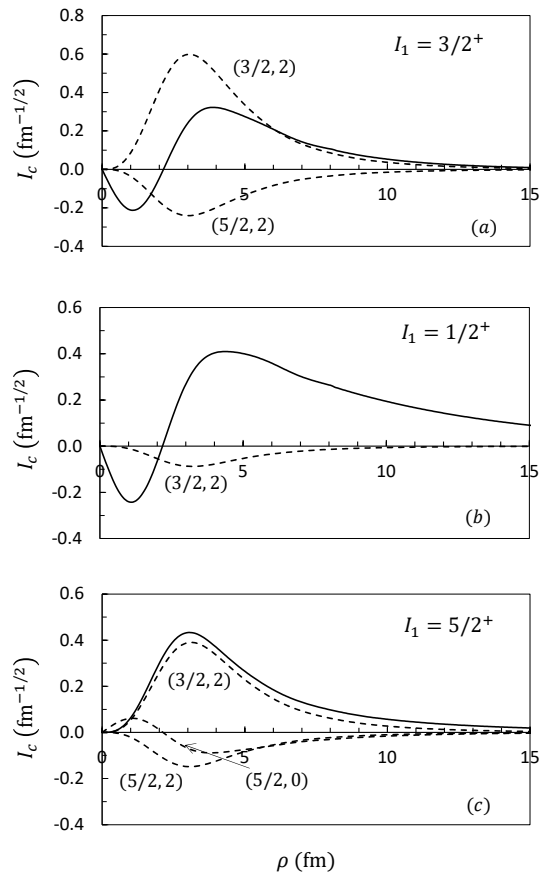


FIG. 1. Overlap integrals of the ^{17}C bound states with spin I_1 . The solid and dashed lines correspond to the $^{16}\text{C}(0^+) + n$ and $^{16}\text{C}(2^+) + n$ configurations, respectively. The labels refer to the $(I\ell)$ values (see also Table I).

responding spectroscopic factors are small, and therefore are not shown here.

B. $^{16}\text{C} + d$ elastic-scattering cross sections

The calculation of the $^{16}\text{C} + d$ scattering wave functions is the first step for the transfer cross sections. The elastic cross section also provides an excellent test of the model. For $^{16}\text{C} + d$, elastic cross sections have been measured at $E_{\text{lab}} = 24 \text{ MeV/nucleon}$ ($E_{\text{c.m.}} = 42.67 \text{ MeV}$) in Ref. [34], which is slightly higher than the energy of the $^{16}\text{C}(d,p)^{17}\text{C}$ experiment (Ref. [19], $E_{\text{c.m.}} = 30.58 \text{ MeV}$). However, this energy difference is not expected to modify the conclusions on the reliability of the model.

The calculation is performed within the CDCC framework, with the Minnesota potential [35] for the $p+n$ interaction. We use a Laguerre basis to describe the deuteron ground state, as well as the $p+n$ pseudostates (see Ref. [36] for detail). Pseudostates up to $E_{\text{max}} = 20 \text{ MeV}$ and $\ell_{\text{max}} = 4$ are included. The $^{16}\text{C} + d$ scattering matrices are computed with the R -matrix formalism [27, 31].

TABLE I. Spectroscopic factors S , ANC (in $\text{fm}^{-1/2}$) and rms radii $\sqrt{\langle r^2 \rangle}$ (in fm) of the ^{17}C bound states (in the first column, the energy is given in MeV). The column $(I\ell)$ refers to the various components in the $^{16}\text{C}(2^+) + n$ channel. The notation x^y stands for $x \times 10^y$.

I_1	$S(0^+)$	$C(0^+)$	(I, ℓ)	$S(2^+)$	$C(2^+)$	$\sqrt{\langle r^2 \rangle}$
$3/2^+$ (-0.734)	5.2^{-3}	7.4^{-3}	(3/2, 0)	0.370	1.596	2.61
			(3/2, 2)	0.972	0.517	
			(5/2, 2)	0.156	-0.205	
$1/2^+$ (-0.517)	0.942	0.959	(3/2, 2)	0.021	-0.080	2.75
			(5/2, 2)	1.1^{-3}	-0.026	
$5/2^+$ (-0.402)	0.562	0.045	(3/2, 2)	0.423	0.290	2.60
			(5/2, 0)	0.029	-0.380	
			(5/2, 2)	0.060	-0.106	

Several tests of the numerical conditions (E_{max} , ℓ_{max} , R -matrix radius, $^{16}\text{C} + d$ basis, etc.) have been performed to check the stability of the cross section. As $^{16}\text{C} + \text{nucleon}$ optical potentials, we use the global parametrizations of Ref. [37] and of Ref. [38], referred to as KD and CH, respectively.

The $^{16}\text{C} + d$ elastic cross section at $E_{\text{c.m.}} = 42.67$ MeV is presented in Fig. 2, with the experimental data of Jiang *et al.* [34]. We show the full CDCC cross sections, as well as the single-channel approximation, where breakup effects of the deuteron are neglected. The minimum near $\theta = 20^\circ$ is well reproduced, and the theoretical cross section is weakly dependent on the $^{16}\text{C} + \text{nucleon}$ optical potential. The present calculation is consistent with results of Ref. [39], where a five-body $^{16}\text{C} + d$ CDCC calculation was performed. It was shown in that reference that breakup effects tend to reduce the cross section for $\theta \gtrsim 30^\circ$. This leads to an underestimation of the cross section, although the shape is consistent with experiment. The availability of experimental data at other energies would be helpful to clarify the role of breakup effects in $^{16}\text{C} + d$ elastic scattering.

C. $^{16}\text{C}(d, p)^{17}\text{C}$ and $^{17}\text{C}(p, d)^{16}\text{C}$ transfer cross sections

Figure 3 presents the $^{16}\text{C}(d, p)^{17}\text{C}$ cross section to the $1/2^+$ and $5/2^+$ states, and compared to experiment [19]. In Ref. [19], the authors compute the cross sections with the Adiabatic Distorted Wave approximation, which involve some parameters. In contrast, the present calculations do not contain any adjustable parameter since the initial state is determined from the $^{16}\text{C} + \text{nucleon}$ potentials, and the ^{17}C final states by the RGM overlap integrals. The spectroscopic factor is not a parameter, but an output of the microscopic model. For both states, the cross sections are weakly dependent on the $^{16}\text{C} + \text{nucleon}$

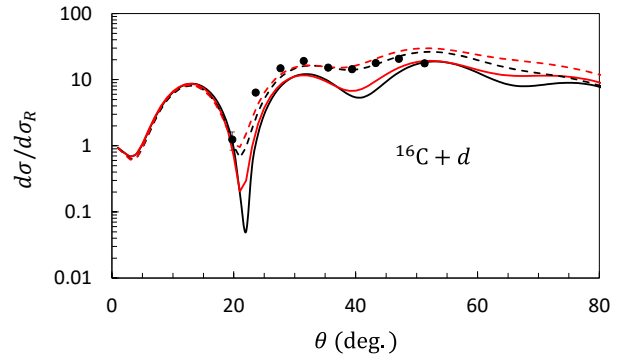


FIG. 2. Elastic $^{16}\text{C} + d$ cross section (divided by the Rutherford cross section) with the CDCC wave functions (solid lines) and with the single-channel approximation (dashed lines). The black and red lines correspond to the KD and CH $^{16}\text{C} + \text{nucleon}$ optical potentials, respectively. Experimental data are taken from Ref. [34]

optical potential, and the CDCC model is in nice agreement with experiment [19], although $^{16}\text{C}(d, p)^{17}\text{C}(1/2^+)$ cross section near the minimum at $\theta \approx 20^\circ$ is overestimated. The single-channel approximation is obviously less good than the full CDCC approach. The quality of the theoretical cross sections, particularly at small angles, supports the spectroscopic factors presented in Table I.

The contribution of the $3/2^+$ ground state, shown in Fig. 4, deserves a special attention. Since this state has a dominant $^{16}\text{C}(2^+) + n$ structure, a standard DWBA approach, using a $^{16}\text{C} + n$ potential of ^{17}C , cannot be used. The spectroscopic factor aims at correcting the normalization of a potential-model wave function. However, if the spectroscopic factor is very small ($S = 5.2 \times 10^{-3}$ in the present case), the shape of the approximated wave function is questionable. Consequently, a microscopic (multichannel) approach is well appropriated for the ^{17}C ground state. The cross section is expected to be small (see Fig. 4) and could not be separated in the experiment of Ref. [19]. Figure 4 suggests that the cross section around $\theta = 0$ is of the order of 0.1 mb, to be compared with 10-20 mb for the excited states. Even if these states contribute very little to the total cross section, a specific measurement would be helpful to assess the validity of the overlap integral provided by the RGM.

Figure 4 also contains the total cross section, where the contribution of the ground and excited ^{17}C states are summed. As mentioned above, the full CDCC calculation agrees reasonably well with experiment, whereas the single-channel approximation underestimates the data for $\theta \gtrsim 10^\circ$.

As the $^{16}\text{C}(d, p)^{17}\text{C}$ cross section to the ground state is small and difficult to measure, we consider the reverse $^{17}\text{C}(p, d)^{16}\text{C}$ reaction. The corresponding cross sections are obtained as explained in Sec. II.C. In practice, we compute the $^{16}\text{C}(2^+)(d, p)^{17}\text{C}$ cross section, and use the detailed balance theorem to deduce the $^{17}\text{C}(p, d)^{16}\text{C}(2^+)$

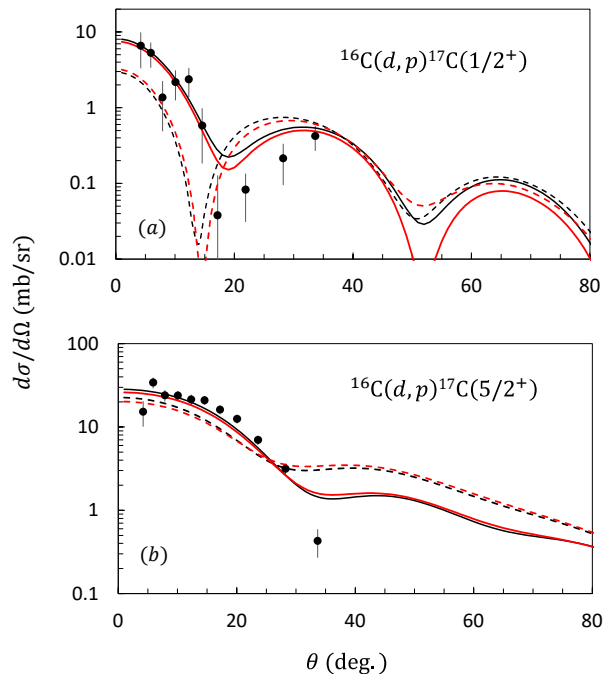


FIG. 3. $^{16}\text{C}(d,p)^{17}\text{C}$ cross sections to the $1/2^+$ (a) and $5/2^+$ (b) states. The solid and dashed lines correspond to the full CDCC calculation, and to the no-breakup approximation, respectively. Results with the KD and CH $^{16}\text{C}+$ nucleon optical potentials are shown in black and red, respectively. The experimental data are taken from Ref. [19], and transformed from the lab frame to the c.m. frame.

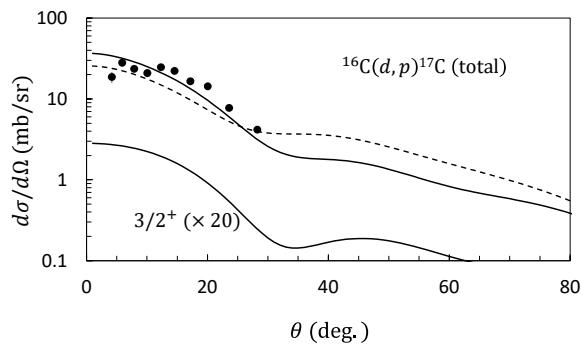


FIG. 4. Ground-state ($\times 20$) and total $^{16}\text{C}(d,p)^{17}\text{C}$ cross sections with the KD potential (the CH results are very similar). See caption to Fig. 3.

values. The $^{17}\text{C} + p$ relative energy is therefore slightly shifted by the Q value ($E_{\text{c.m.}} = 29.1$ MeV). The cross sections to the 0^+ and 2^+ states are shown in Fig. 5. The calculation of the $^{16}\text{C}(2^+)(d,p)^{17}\text{C}$ cross section is similar to the previous $^{16}\text{C}(0^+)(d,p)^{17}\text{C}$ calculation, but is sensitive to the $^{16}\text{C}(2^+) + n$ overlap integral of ^{17}C . The nucleon+ ^{16}C optical potentials are unchanged.

The 2^+ contribution is of the order of 10 mb at small angles, similar to the values found for $^{16}\text{C}(d,p)^{17}\text{C}$. As

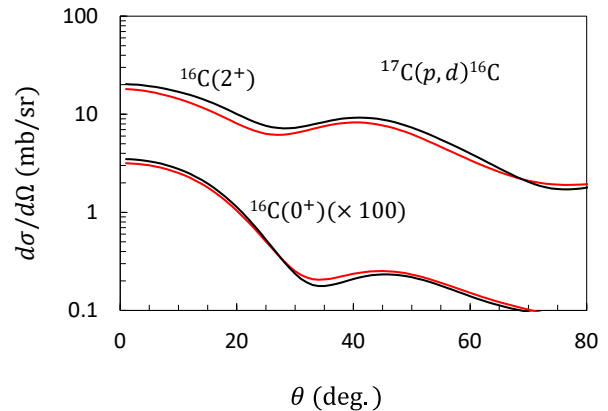


FIG. 5. $^{17}\text{C}(p,d)^{16}\text{C}$ cross sections to the 0^+ and 2^+ states of ^{16}C at $E_{\text{c.m.}} = 29.1$ MeV (see text). The black and red lines correspond to the KD and CH $^{16}\text{C}+$ nucleon optical potentials.

expected, the 0^+ is small, and lower and 0.1 mb. However, such a measurement would be a stringent test of the RGM, as it would probe a small component of the ^{17}C wave function, more sensitive to coupling effects. As for the $^{16}\text{C}(d,p)^{17}\text{C}$ cross sections, the sensitivity to the optical potential is low.

IV. CONCLUSION

We have analyzed recent data on the $^{16}\text{C}(d,p)^{17}\text{C}$ reaction [19] by using microscopic ^{17}C wave functions. In the microscopic RGM formalism, the wave functions are fully antisymmetric. The $^{16}\text{C} + n$ cluster structure includes many ^{16}C states, which provides a realistic description of the low-lying states. The long-range behavior is treated by the R -matrix methods, for bound states as well as for scattering states. The $^{16}\text{C} + d$ wave functions are obtained within the CDCC approach, which includes deuteron breakup effects. We have shown that these effects are not negligible in the transfer cross sections.

The transfer cross sections are in fair agreements with experiment, without any adjustable parameter. We have confirmed that the $^{16}\text{C}(d,p)^{17}\text{C}(\text{gs})$ cross section is small, owing to the dominant $^{16}\text{C}(2^+) + n$ structure of the ^{17}C ground state. We have determined the reverse $^{17}\text{C}(p,d)^{16}\text{C}$ cross section, and shown that ^{16}C would be essentially populated in the 2^+ first excited state. A measurement of the cross sections, and in particular of the branching ratio, should provide a strong test of the RGM wave function.

ACKNOWLEDGMENTS

We are grateful to B. Fernández-Domínguez for providing us with the cross section data of Ref. [19]. This

work was supported by the Fonds de la Recherche Sci-

entifique - FNRS under Grant Numbers 4.45.10.08 and J.0065.22.

-
- [1] I. Tanihata, H. Savajols, and R. Kanungo, *Prog. Part. Nucl. Phys.* **68**, 215 (2013).
- [2] T. Otsuka, A. Gade, O. Sorlin, T. Suzuki, and Y. Utsuno, *Rev. Mod. Phys.* **92**, 015002 (2020).
- [3] Y. Blumenfeld, T. Nilsson, and P. Van Duppen, *Physica Scripta* **2013**, 014023 (2013).
- [4] U. Datta Pramanik, T. Aumann, K. Boretzky, B. Carlson, D. Cortina, T. Elze, H. Emling, H. Geissel, A. Grünschloß, M. Hellström, S. Ilievski, J. Kratz, R. Kulesa, Y. Leifels, A. Leistenschneider, E. Lubkiewicz, G. Münzenberg, P. Reiter, H. Simon, K. Sümmerner, E. Wajda, and W. Walus, *Phys. Lett. B* **551**, 63 (2003).
- [5] Z. Elekes, Z. Dombrádi, R. Kanungo, H. Baba, Z. Fülöp, J. Gibelin, A. Horváth, E. Ideguchi, Y. Ichikawa, N. Iwasa, H. Iwasaki, S. Kanno, S. Kawai, Y. Kondo, T. Motobayashi, M. Notani, T. Ohnishi, A. Ozawa, H. Sakurai, S. Shimoura, E. Takeshita, S. Takeuchi, I. Tanihata, Y. Togano, C. Wu, Y. Yamaguchi, Y. Yanagisawa, A. Yoshida, and K. Yoshida, *Phys. Lett. B* **614**, 174 (2005).
- [6] H. G. Bohlen, R. Kalpakchieva, W. von Oertzen, T. N. Massey, A. A. Ogloblin, G. de Angelis, M. Milin, C. Schulz, T. Kokalova, and C. Wheldon, *Eur. J. Phys. A* **31**, 279 (2007).
- [7] H. Ueno, H. Miyatake, Y. Yamamoto, S. Tanimoto, T. Shimoda, N. Aoi, K. Asahi, E. Ideguchi, M. Ishihara, H. Izumi, T. Kishida, T. Kubo, S. Mitsuoka, Y. Mizoi, M. Notani, H. Ogawa, A. Ozawa, M. Sasaki, T. Shirakura, N. Takahashi, and K. Yoneda, *Phys. Rev. C* **87**, 034316 (2013).
- [8] Y. Satou, T. Nakamura, N. Fukuda, T. Sugimoto, Y. Kondo, N. Matsui, Y. Hashimoto, T. Nakabayashi, T. Okumura, M. Shinohara, T. Motobayashi, Y. Yanagisawa, N. Aoi, S. Takeuchi, T. Gomi, Y. Togano, S. Kawai, H. Sakurai, H. Ong, T. Onishi, S. Shimoura, M. Tamaki, T. Kobayashi, H. Otsu, Y. Matsuda, N. Endo, M. Kitayama, and M. Ishihara, *Phys. Lett. B* **660**, 320 (2008).
- [9] D. Smalley, H. Iwasaki, P. Navrátil, R. Roth, J. Langhammer, V. M. Bader, D. Bazin, J. S. Berryman, C. M. Campbell, J. Doherty, P. Fallon, A. Gade, C. Langer, A. Lemasson, C. Loelius, A. O. Macchiavelli, C. Morse, J. Parker, S. Quaglioni, F. Recchia, S. R. Stroberg, D. Weisshaar, K. Whitmore, and K. Wimmer, *Phys. Rev. C* **92**, 064314 (2015).
- [10] S. Kim, J. Hwang, Y. Satou, N. Orr, T. Nakamura, Y. Kondo, J. Gibelin, N. Achouri, T. Aumann, H. Baba, F. Delaunay, P. Doornenbal, N. Fukuda, N. Inabe, T. Isobe, D. Kameda, D. Kanno, N. Kobayashi, T. Kobayashi, T. Kubo, S. Leblond, J. Lee, F. Marqués, R. Minakata, T. Motobayashi, D. Murai, T. Murakami, K. Muto, T. Nakashima, N. Nakatsuka, A. Navin, S. Nishi, S. Ogoshi, H. Otsu, H. Sato, Y. Shimizu, H. Suzuki, K. Takahashi, H. Takeda, S. Takeuchi, R. Tanaka, Y. Togano, A. Tuff, M. Vandebrouck, and K. Yoneda, *Phys. Lett. B* **836**, 137629 (2023).
- [11] K. Amos, L. Canton, P. Fraser, S. Karataglidis, J. Svenne, and D. van der Knijff, *Nucl. Phys. A* **879**, 132 (2012).
- [12] P. Descouvemont, *Nucl. Phys. A* **675**, 559 (2000).
- [13] N. K. Timofeyuk and P. Descouvemont, *Phys. Rev. C* **81**, 051301 (2010).
- [14] K. Wildermuth and Y. C. Tang, *A Unified Theory of the Nucleus*, edited by K. Wildermuth and P. Kramer (Vieweg, Braunschweig, 1977).
- [15] H. Horiuchi, *Prog. Theor. Phys. Suppl.* **62**, 90 (1977).
- [16] D. Baye and N. K. Timofeyuk, *Phys. Lett. B* **293**, 13 (1992).
- [17] G. R. Satchler, *Direct Nuclear Reactions* (Oxford University Press, 1983).
- [18] N. Timofeyuk and R. Johnson, *Prog. Part. Nucl. Phys.* **111**, 103738 (2020).
- [19] X. Pereira-López, B. Fernández-Domínguez, F. Delaunay, N. Achouri, N. Orr, W. Catford, M. Assié, S. Bailey, B. Bastin, Y. Blumenfeld, R. Borcea, M. C. oo, L. Caceres, E. Clément, A. Corsi, N. Curtis, Q. Deshayes, F. Farget, M. Fisichella, G. de France, S. Franchoo, M. Freer, J. Gibelin, A. Gillibert, G. Grinyer, F. Hammache, O. Kamalou, A. Knapton, T. Kokalova, V. Lapoux, J. Lay, B. L. Crom, S. Leblond, J. Lois-Fuentes, F. Marqués, A. Matta, P. Morfouace, A. Moro, T. Otsuka, J. Pancin, L. Perrot, J. Piot, E. Pollacco, D. Ramos, C. Rodríguez-Tajes, T. Roger, F. Rotaru, M. Sénoville, N. de Séreville, R. Smith, O. Sorlin, M. Stanoiu, I. Stefan, C. Stodel, D. Suzuki, T. Suzuki, J. Thomas, N. Timofeyuk, M. Vandebrouck, J. Walshe, and C. Wheldon, *Phys. Lett. B* **811**, 135939 (2020).
- [20] P. Descouvemont, *Eur. Phys. J. A* **58**, 193 (2022).
- [21] M. Yahiro, T. Matsumoto, K. Minomo, T. Sumi, and S. Watanabe, *Prog. Theor. Phys. Supp.* **196**, 87 (2012).
- [22] M. Gomez-Ramos and A. M. Moro, *Phys. Rev. C* **95**, 044612 (2017).
- [23] P. Descouvemont, *Phys. Lett. B* **772**, 1 (2017).
- [24] N. K. Timofeyuk, *J. Phys. G* **41**, 094008 (2014).
- [25] N. K. Timofeyuk, *J. Phys. G* **48**, 015105 (2020).
- [26] P. Descouvemont and M. Dufour, *Clusters in nuclei*, vol. 2 (Springer Berlin Heidelberg, 2012) Chap. Microscopic Cluster Models, pp. 1–66.
- [27] P. Descouvemont and D. Baye, *Rep. Prog. Phys.* **73**, 036301 (2010).
- [28] P. Descouvemont, *Phys. Rev. C* **107**, 014312 (2023).
- [29] DLMF, *NIST Digital Library of Mathematical Functions*, <https://dlmf.nist.gov/>, F. W. J. Olver, A. B. Olde Daalhuis, D. W. Lozier, B. I. Schneider, R. F. Boisvert, C. W. Clark, B. R. Miller, B. V. Saunders, H. S. Cohl, and M. A. McClain, eds.
- [30] P. Burke, *R-Matrix Theory of Atomic Collisions. Application to Atomic, Molecular and Optical Processes*, Springer Series on Atomic, Optical, and Plasma Physics, Vol. 61 (Springer, 2011).
- [31] P. Descouvemont, *Comput. Phys. Commun.* **200**, 199 (2016).
- [32] Shubhchintak and P. Descouvemont, *Phys. Rev. C* **100**, 034611 (2019).

- [33] A. Dobrovolsky, G. Korolev, S. Tang, G. Alkhazov, G. Colò, I. Dillmann, P. Egelhof, A. Estradé, F. Farinon, H. Geissel, S. Ilieva, A. Inglessi, Y. Ke, A. Khanzadeev, O. Kiselev, J. Kurcewicz, L. Chung, Y. Litvinov, G. Petrov, A. Prochazka, C. Scheidenberger, L. Sergeev, H. Simon, M. Takechi, V. Volkov, A. Vorobyov, H. Weick, and V. Yatsoura, *Nucl. Phys. A* **1008**, 122154 (2021).
- [34] Y. Jiang, J. L. Lou, Y. L. Ye, Y. Liu, Z. W. Tan, W. Liu, B. Yang, L. C. Tao, K. Ma, Z. H. Li, Q. T. Li, X. F. Yang, J. Y. Xu, H. Z. Yu, J. X. Han, S. W. Bai, S. W. Huang, G. Li, H. Y. Wu, H. L. Zang, J. Feng, Z. Q. Chen, Y. D. Chen, Q. Yuan, J. G. Li, B. S. Hu, F. R. Xu, J. S. Wang, Y. Y. Yang, P. Ma, Q. Hu, Z. Bai, Z. H. Gao, F. F. Duan, L. Y. Hu, J. H. Tan, S. Q. Sun, Y. S. Song, H. J. Ong, D. T. Tran, D. Y. Pang, and C. X. Yuan (RIBLL Collaboration), *Phys. Rev. C* **101**, 024601 (2020).
- [35] D. R. Thompson, M. LeMere, and Y. C. Tang, *Nucl. Phys. A* **286**, 53 (1977).
- [36] T. Druet, D. Baye, P. Descouvemont, and J.-M. Sparenberg, *Nucl. Phys. A* **845**, 88 (2010).
- [37] A. J. Koning and J. P. Delaroche, *Nucl. Phys. A* **713**, 231 (2003).
- [38] R. L. Varner, W. J. Thompson, T. L. McAbee, E. J. Ludwig, and T. B. Clegg, *Phys. Rep.* **201**, 57 (1991).
- [39] Shubhchintak and P. Descouvemont, *Phys. Rev. C* **105**, 024605 (2022).